

# Extraordinary role of $\text{Ca}^{2+}$ ions on the magnetization of $\text{LaFeO}_3$ orthoferrite

M.A. Ahmed\*, S.I. El-Dek

*Materials Science Lab (1), Physics Department, Faculty of Science, Cairo University, Giza, Egypt*

Received 18 November 2004; received in revised form 1 October 2005; accepted 3 November 2005

## Abstract

Samples of  $\text{La}_{1-x}\text{Ca}_x\text{FeO}_3$  were synthesized in air for  $0.05 \leq x \leq 0.55$ . X-ray powder diffraction analysis showed that the samples were formed in a single phased orthorhombic structure ( $Pbnm$ ) where the lattice parameters were calculated and reported. The dc magnetic susceptibility was measured using Faraday's method from room temperature up to about 850 K at five different magnetic field intensities. The obtained results showed that the samples were antiferromagnetic with slight canting of the  $\text{Fe}^{3+}$  spins. The substitution of  $\text{La}^{3+}$  by  $\text{Ca}^{2+}$  ions lowers the Néel temperature. The calculated values of the effective magnetic moment as a function of the  $\text{Ca}^{2+}$  concentration were in good agreement with the reported data. The results were interpreted on the basis of the charge difference and the ionic radii of the  $\text{La}^{3+}$  and  $\text{Ca}^{2+}$  ions.  
© 2005 Elsevier B.V. All rights reserved.

**Keywords:** Orthoferrite; Structural distortion; Magnetization

## 1. Introduction

The perovskite type oxides [1] have the general formula  $\text{ABO}_3$  with A representing a large cation, usually rare earth ion, while B is the smaller one. The perovskite structure can be described as a framework of corner-sharing  $\text{BO}_6$  octahedron that contains A cations at 12-coordinate sites. Amongst the perovskite compounds, there are the  $\text{A}^{3+}\text{B}^{3+}$  or (3–3) perovskites, in their orthorhombic forms, the displacement of different  $\text{A}^{3+}$  cations from the ideal positions appears to decrease with increasing the size of  $\text{A}^{3+}$  with the same  $\text{B}^{3+}$  cation [2].

Recently, it was found that the rare earth orthoferrites [3] ( $\text{RFeO}_3$ ) with perovskite type structure are interesting materials for most of electronic applications because of their mixed conductivity [4]. These materials display ionic and electronic defects [5], which make them important candidates for the development of solid-oxide fuel cells [6], active catalysis for oxidation or reduction of pollutant gases [7,8], oxygen sensor electrodes [9,10], gas diffusion electrodes, oxygen permeation membranes [11–13], chemical sensors for the detection of humidity [14], alcohol [15] and gases [16–18] such as oxygen [19,20], CO [21,22], and  $\text{NO}_2$  [23–25] as well as environmental monitoring applications [26].

The remarkable magnetic properties of the rare earth orthoferrite family of crystals ( $\text{RFeO}_3$ ) have attracted continued experimental and theoretical interests [27]. For example, they were the first group of materials to be considered in bubble memory applications for computer design [28]. The direct magnetic interaction between nearest neighbors  $\text{Fe}^{3+}$  moments in this case is negligible. Instead, the spins are coupled through the oxygen ions by the mechanism of super exchange interaction. This interaction is predominantly antiferromagnetic; however, it has an antisymmetric component that causes a slight canting of the moments of adjacent iron atoms and a resultant weak ferromagnetic moment as well [29].

The importance of orthoferrites in many applications encourages us to through light on the role of  $\text{Ca}^{2+}$  ions substitution on the crystal structure and magnetic characterizations of  $\text{LaFeO}_3$  by X-ray diffraction and magnetic susceptibility. Also, one of our goals is to study the solubility limit of  $\text{Ca}^{2+}$  ions in the  $\text{LaFeO}_3$  matrix in order to improve the physicochemical properties of the compound to be more applicable.

## 2. Experimental techniques

Samples of  $\text{La}_{1-x}\text{Ca}_x\text{FeO}_3$  ( $0.05 \leq x \leq 0.55$ ) were prepared by the conventional solid-state reaction from oxides of analar grade form (BDH),  $\text{La}_2\text{O}_3$ , CaO and  $\text{Fe}_2\text{O}_3$ . Stoichiometric ratios were good mixed, grinded using agate mortar for 3 h and

\* Corresponding author. Tel.: +20 25676742; fax: +20 25727556.  
E-mail address: moala47@hotmail.com (M.A. Ahmed).

transferred to electric ball mill for another 3 h. The samples were pressed into pellets form using uniaxial press of pressure  $5 \times 10^8 \text{ N/m}^2$ . The pellets were presintered in air at  $950^\circ\text{C}$  for 20 h with a heating rate of  $1^\circ\text{C}/\text{min}$ . They were cooled to room temperature with the same rate as that of heating, regrinded and pressed again into pellets. The pellets were fired at  $1200^\circ\text{C}$  for 30 h at the same previous rate and then cooled to room temperature with the same rate as that of heating. Regrinding was carried out again, then the powder was sieved and pressed into discs of diameter 1 cm and thickness of  $\cong 1.5 \text{ mm}$ , fired at  $1200^\circ\text{C}$  for another 30 h in air with the same rate of heating.

The samples were checked by X-ray diffraction analysis using Philips Diffractometer model “PW3710” with a Cu target of wave length ( $\lambda = 1.54060 \text{ \AA}$ ) to assure the complete solid-state reaction. Indexing of the obtained diffraction patterns using JCPDS cards was done and the lattice parameters were calculated using the computer program Treor [30].

The dc magnetic susceptibility measurements were carried out using Faraday’s method in which a very small amount of the powdered sample was inserted in a cylindrical glass tube at the point of maximum gradient. The measurements were performed from room temperature up to  $\cong 850 \text{ K}$  at five different values of magnetic field intensity ranging from 833 to 3800 Oe.

### 3. Results and discussion

#### 3.1. X-ray analysis

X-ray diffraction analysis, Fig. 1, of the samples of  $\text{La}_{1-x}\text{Ca}_x\text{FeO}_3$  ( $0.05 \leq x \leq 0.55$ ), reveals single-phase orthorhombic structure with space group ( $Pbnm$ ). At  $x = 0.55$ , a small intensity of a secondary phase appeared which was identified as CaO. The variation of the lattice parameters with Ca content is illustrated in Fig. 1, from which it is clear that the value of  $b$  is nearly constant with increasing  $x$  up to 0.35, after that it decreases giving a minimum at  $x = 0.45$  and increases again. The trend of both parameters  $a$  and  $c$  is nearly the same, where they reach a maximum value at  $x = 0.45$  corresponding to the minimum of  $b$  and then decrease. This result reflects the distortion that takes place in the lattice at  $x = 0.45$  due to the mismatch between the size of the  $\text{La}^{3+}$  and  $\text{Ca}^{2+}$  ions. Also, the peculiar change of the

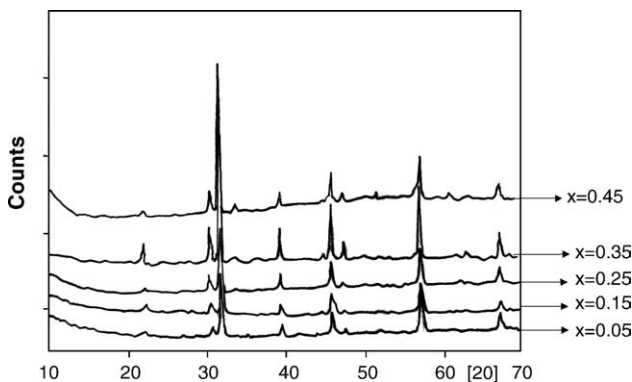


Fig. 1. X-ray diffraction patterns for the samples  $\text{La}_{1-x}\text{Ca}_x\text{FeO}_3$  ( $0.05 \leq x \leq 0.55$ ).

lattice parameters at  $x = 0.45$  is directly related to the generation of a relatively large amount of  $\text{Fe}^{4+}$  ions instead of  $\text{Fe}^{3+}$  ions as the result of increasing  $\text{Ca}^{2+}$  content. The chemical formula could then be written as [31]  $\text{La}_{1-x}\text{Ca}_x\text{Fe}_{1-t}^{3+}\text{Fe}_t^{4+}\text{O}_{3-y}$  where  $t \leq x$ ,  $0 \leq t \leq 0.07$ . These results are in good agreement with those reported by Komornicki et al. [31].

The tolerance factor ( $t$ ) Eq. (1) [32], is a geometrical factor characterizing the size mismatch that occurs when the A-site cations are too small to fill the space in the three dimensional network of  $\text{BO}_6$  octahedra:

$$t = \frac{R_A + R_O}{\sqrt{2}(R_B + R_O)} \quad (1)$$

$R_A$ ,  $R_B$  and  $R_O$  are the ionic radii of the A, B and oxygen ions, respectively, in the  $\text{ABO}_3$  perovskite. The effective ionic radius of the A-cation is calculated from the relation [3]:

$$R_{\text{eff}} = (1 - x)R_{\text{La}^{3+}} + xR_{\text{Ca}^{2+}} \quad [32] \quad (2)$$

When the tolerance factor decreases, the orthorhombic distortion increases. On the other hand, the  $\theta_{\text{B-O-B}}$  angle, which is a measure of the tilting of the octahedron, is directly correlated to the cell distortion,  $\theta$  decreases when the distortion increases [32]. The ideal perovskite structure has  $t = 1$ , where the orthorhombic distorted perovskite structure has  $t \cong 0.8$ . In the investigated samples, the iron is the B cation; increasing  $\text{Ca}^{2+}$  content decreases the tolerance factor from  $t = 0.902$  at  $x = 0.05$  to  $t = 0.895$  at  $x = 0.55$ , assuming nine-fold coordination A-cation. This means that the orthorhombic distortion increases with  $\text{Ca}^{2+}$  content which agrees well with the variation of the lattice parameters, Fig. 2, as the Ca content increases.

#### 3.2. Magnetic susceptibility

The dependence of the molar magnetic susceptibility on the absolute temperature as a function of the magnetic field intensity for the sample  $\text{La}_{1-x}\text{Ca}_x\text{FeO}_3$  ( $x = 0.25$ ) is shown in Fig. 3(a) as a typical curve. The data in the figure shows stability in  $\chi_M$  from 900 down to  $\cong 690 \text{ K}$ , below which, a sudden increase in  $\chi_M$  is observed with the continuous decrease in temperature. The value of  $\chi_M$  at room temperature is  $\cong 6$  times its value at 690 K. The intensity of the magnetic field affects directly on the values of  $\chi_M$  where it decreases with increasing the intensity of the magnetic field.

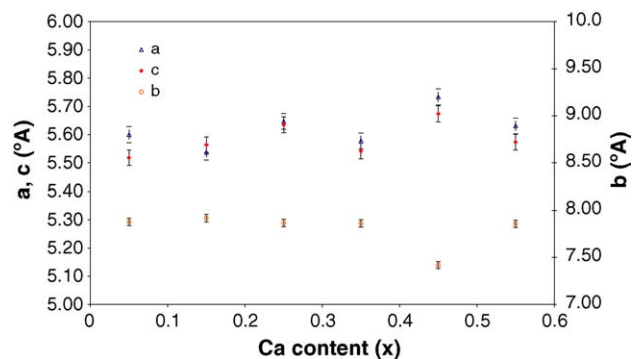


Fig. 2. Variation of the lattice parameters  $a$ ,  $b$  and  $c$  with the Ca content ( $x$ ).

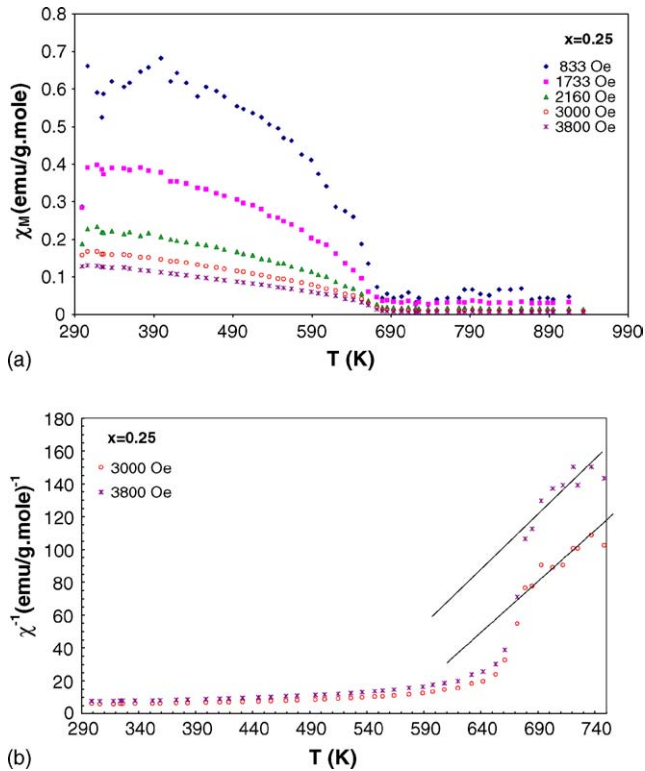


Fig. 3. (a) The dependence of the molar magnetic susceptibility ( $\chi_M$ ) on the absolute temperature for the sample with  $x=0.25$  as a function of magnetic field intensities as a typical curve; (b) the dependence of the reciprocal of the molar magnetic susceptibility ( $\chi_M^{-1}$ ) on the absolute temperature for the sample with  $x=0.25$  as a function of magnetic field intensities as a typical curve.

The magnetic susceptibility data obeys the Curie–Weiss law below the Néel temperature, while above  $T_N$  the sample behaves like a normal paramagnet obeying the Curie law, Fig. 3(b). The values of the magnetic constants were calculated from the plot of  $\chi^{-1}$  versus  $T$  (Fig. 3(b)). Below the Néel temperature,  $T_N=693$  K at  $x=0.25$ ; the magnetic ordering of  $\text{Fe}^{3+}$  ions in orthoferrites is that of a canted antiferromagnet of the G-type [33]. At room temperature, the net moments of  $\text{Fe}^{3+}$  ions lie along the  $c$ -axis whereas the sublattice moments ( $G$ ) lie in  $(a,b)$  plane being slightly canted to the  $a$ -axis. Above the Néel temperature, the samples behave as completely paramagnetic [34].

Depending mainly on the synthesis techniques and conditions (sintering atmosphere, cooling rate, etc.) and the difference in ionic radii between  $\text{La}^{3+}$  ( $r_{\text{ionic}}=1.216$  Å) and  $\text{Ca}^{2+}$  ions ( $r_{\text{ionic}}=1.180$  Å) in nine-fold coordination, the substitution of  $\text{La}^{3+}$  by  $\text{Ca}^{2+}$  in  $\text{LaFeO}_3$  has at least two possibilities. First: the system  $\text{La}_{1-x}\text{Ca}_x\text{FeO}_3$  consists of two or more phases; iron possesses an intermediate valence state that increases gradually from  $\text{Fe}^{3+}$  to  $\text{Fe}^{4+}$  with increasing  $x$ . The second possibility is that the iron keeps its stable trivalent state and the oxygen deficiency appears in the lattice in order to neutralize the compound electrically.

Fig. 4 represents the variation of the calculated effective magnetic moment ( $\mu_{\text{eff}}$ ), the Curie constant ( $C$ ) and the Néel temperature ( $T_N$ ) as a function of the calcium content. The decrease of the Néel temperature is probably due to the fact

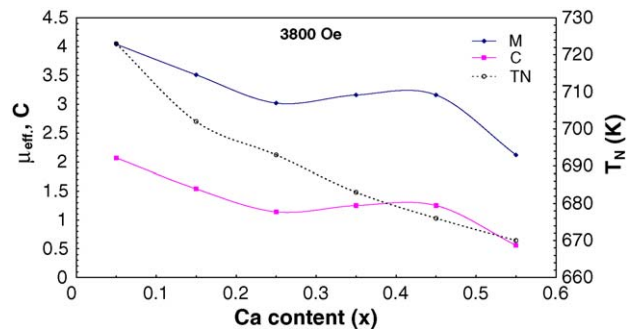


Fig. 4. Variation of the effective magnetic moment ( $\mu$ ) in B.M., the Curie constant ( $C$ ) in (emu/g mol) K at 3800 Oe and the Néel temperature ( $T_N$ ) in K with the Ca content ( $x$ ).

that increasing  $\text{Ca}^{2+}$  content in the solid solution increases the number of  $\text{Fe}^{4+}$  ( $3d^4$ ) and decreases the number of  $\text{Fe}^{3+}$  ( $3d^5$ ). This expectation is enhanced by the decrease in the effective magnetic moment with increasing  $\text{Ca}^{2+}$  concentration. The possible explanation is that the  $\text{Fe}^{3+}$  ( $3d^5$ ) ions have the largest magnetic moment (5.85 B.M.) as compared with that of iron ions in another valence state [35]. This means that, with increasing  $x$ , the number of  $\text{Fe}^{4+}$  ( $3d^4$ ), of lower magnetic moment, increases:

Theoretically, the effective magnetic moment of the investigated samples can be calculated using the formula [36]:

$$\mu_{\text{eff}} = ((1-x)\mu_{\text{La}^{3+}}^2 + x\mu_{\text{Ca}^{2+}}^2 + (1-t)\mu_{\text{Fe}^{3+}}^2 + t\mu_{\text{Fe}^{4+}}^2)^{1/2}$$

As, the  $\text{La}^{3+}$  and  $\text{Ca}^{2+}$  ions are diamagnetic, therefore their net magnetic moments are too small so they can be neglected. The resultant is that of the iron ions, in the investigated samples, taking into consideration that iron exists in two different valence states. The dependence of  $\mu_{\text{eff}}$  on  $x$  is mainly due to ratio of ( $\text{Fe}^{4+}/\text{Fe}^{3+}$ ) ions due to the increase of  $\text{Ca}^{2+}$  ions. It was reported that [35]  $\mu_{\text{eff}}$  is calculated for the metal ion from  $\mu_{\text{eff}} = g\sqrt{J(J+1)}$ ; where  $g$  is the Landau splitting factor and  $J$  is the total angular momentum; which is equal to 5.85 B.M. for  $\text{Fe}^{3+}$  ions. This value agrees with the experimental calculated value ( $\mu_{\text{eff}} = 2.83\sqrt{C}$ ,  $C$  is the Curie constant) from ( $\chi^{-1}$  versus  $T$ ) at  $x=0.05$  (6.20 B.M.) at 833 Oe. The difference here is due to the canted antiferromagnetic character of the samples.

The influence of the tolerance factor ( $t$ ) on the magnetic properties is well established [37,38] for super exchange antiferromagnets such as  $\text{LaFeO}_3$ . Analysis of this system has shown that the Néel temperature is directly proportional to  $\cos^2 \theta$ . Consequently, one can attribute the decrease of the Néel temperature with increasing  $\text{Ca}^{2+}$  content to the decrease of the tolerance factor.

The variation of the molar magnetic susceptibility with the absolute temperature at different  $\text{Ca}^{2+}$  contents is illustrated in Fig. 5. The remarkable increase in  $\chi_M$  with increasing  $\text{Ca}^{2+}$  ion content is explained by the increase in the number of  $\text{Fe}^{4+}$  ions on the expense of  $\text{Fe}^{3+}$ , thus giving rise to a high probability of the super exchange interaction between  $\text{Fe}^{3+}$  and  $\text{Fe}^{4+}$  where they are antiferromagnetically coupled through the oxygen anions.

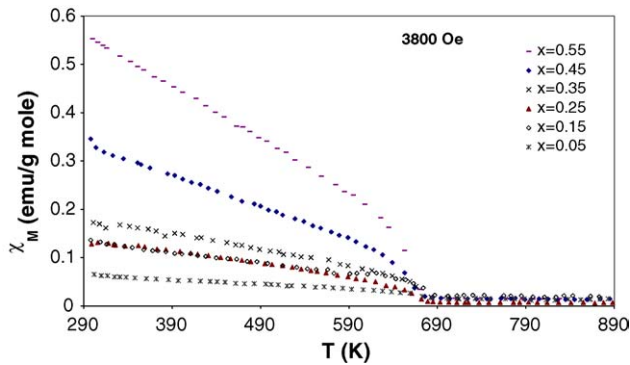


Fig. 5. The dependence of the molar magnetic susceptibility ( $\chi_M$ ) on the absolute temperature at different Ca concentrations.

#### 4. Conclusion

X-ray diffraction analysis for the investigated samples reveals single-phase orthorhombic structure. The trend of the lattice parameters  $a$ ,  $b$  and  $c$  as a function of Ca content is the same for  $a$  and  $c$  with the reverse trend for  $b$ . This reflects the distortion occurred in the lattice at  $x = 0.45$ . The value of the effective magnetic moment and the other magnetic constants decrease with increasing Ca content. This enhances the presence of  $\text{Fe}^{4+}$  on the expense of  $\text{Fe}^{3+}$  ions in the samples, where the two ions are coupled antiferromagnetically through oxygen anions.

#### References

- [1] K. Ito, K. Tezuka, Y. Hinatsu, J. Solid State Chem. 157 (2001) 173–179.
- [2] S. Geller, Acta Crystallogr. 10 (1975) 243.
- [3] E. Traversa, P. Nunziante, L. Sagletti, B. Allieri, L.E. Depero, H. Aono, Y. Sadaoka, J. Am. Ceram. Soc. 83 (5) (2000) 1087–1092.
- [4] J.W. Stevenson, T.R. Armstrong, R.D. Carnein, L.D. Pederson, W.J. Weba, J. Electrochem. Soc. 143 (1996) 2722–2729.
- [5] M. Cherry, M.S. Islam, C.R.A. Catlow, J. Solid State Chem. 118 (1995) 125–132.
- [6] N.Q. Minh, J. Am. Ceram. Soc. 76 (1993) 563–568.
- [7] J.G. McCarty, H. Wise, Catal. Today 8 (1990) 231–248.
- [8] K. Tabata, M. Misono, Catal. Today 8 (1990) 249–261.
- [9] T. Inoue, N. Seki, K. Eguschi, H. Arai, J. Electrochem. Soc. 137 (1990) 2523–2527.
- [10] C.B. Aleock, R.C. Doshi, Y. Shen, Solid State Ionics 51 (1992) 281.
- [11] G. Karlsson, Electrochim. Acta 30 (1985) 1555–1561.
- [12] Y. Teraoka, T. Nobunaga, N. Yamazoe, Chem. Lett. (1988) 503–506.
- [13] J.M. Bouwmeester, H. Kruidhof, A.J. Burggraf, Solid State Ionics 72 (1994) 185–194.
- [14] Y. Shimizu, M. Shimabukuro, H. Arai, T. Seiyama, Chem. Lett. (1985) 917–920.
- [15] H. Obayashi, T. Kudo, Nippon Kagaku Kaishi (1980) 1568–1572.
- [16] T. Arakawa, H. Kurachi, J. Shiokawa, J. Mater. Sci. 4 (1985) 1207–1210.
- [17] M.C. Carotta, M.A. Buatrurri, G. Martinelli, Y. Sadaoka, P. Nunziante, E. Traversa, Sens. Actuators B 44 (1997) 590–594.
- [18] M.C. Carotta, G. Martinelli, Y. Sadaoka, P. Nunziante, E. Traversa, Sens. Actuators B 48 (1998) 270–276.
- [19] C. Yu, Y. Shimizu, H. Arai, Chem. Lett. (1986) 563–566.
- [20] M.L. Post, B.W. Sanders, P. Kennepohl, Sens. Actuators B 13 (1993) 272–275.
- [21] W.B. Li, H. Yoneyama, H. Tamura, Nippon Kagaku Kaishi (1982) 761–767.
- [22] Y. Takahashi, H. Taguchi, J. Mater. Sci. Lett. 3 (1984) 251–253.
- [23] Y. Matsuura, S. Matsushima, M. SaKamoto, Y. Sadaoka, J. Mater. Chem. 3 (1993) 767.
- [24] E. Traversa, S. Matsushima, G. Okada, Y. Sadaoka, Y. Sakai, K. Watanabe, Sens. Actuators B 25 (1995) 661–664.
- [25] E. Traversa, S. Villanti, G. Gusmano, H. Aono, Y. Sadaoka, J. Am. Ceram. Soc. 82 (1999) 2442–2450.
- [26] G. Martinelli, M. Carotta, M. Ferroni, Y. Sadaoka, E. Traversa, Sens. Actuators B 55 (1999) 99–110.
- [27] S. Venugopalan, M. Dutta, A.K. Ramdas, J.P. Remeika, Phys. Rev. B 31 (3) (1985) 1490.
- [28] A.H. Bobeck, E. Della Torre, Magnetic Bubbles, Amsterdam, North-Holland, 1975 (Chapter 4).
- [29] D. Treves, J. Appl. Phys. 36 (1965) 1033.
- [30] P.E. Werner, Treor, Trial and Error Program for Indexing Unknown Powder Patterns, University of Stockholm, Stockholm, Sweden, 1984.
- [31] S. Komornicki, L. Fournes, J.-C. Grenier, F. Menil, M. Pouchard, P. Hagenmuller, Mater. Res. Bull. 16 (8) (1981) 967–973.
- [32] K. Tezuka, Y. Hinatsu, J. Solid State Chem. 141 (1998) 404–410.
- [33] J.L. Garcia-Munoz, J. Rodriguez Carvajal, Phys. Rev. B 46 (8) (1992) 4414.
- [34] I. Sosnowska, P. Fische, Am. Phys. Inst. (API) 89 (1982) 346.
- [35] L.F. Bates, Modern Magnetism, Cambridge University Press, 1948.
- [36] A.J. Dekker, Solid State Physics, vol. 450, Prentice-Hall, New York, 1970.
- [37] D. Treves, M. Eibschutz, P. Coppens, Phys. Lett. 18 (1965) 216.
- [38] G.A. Sawatzky, W. Geertsma, C. Haas, J. Magn. Magn. Mater. 3 (1976) 37.